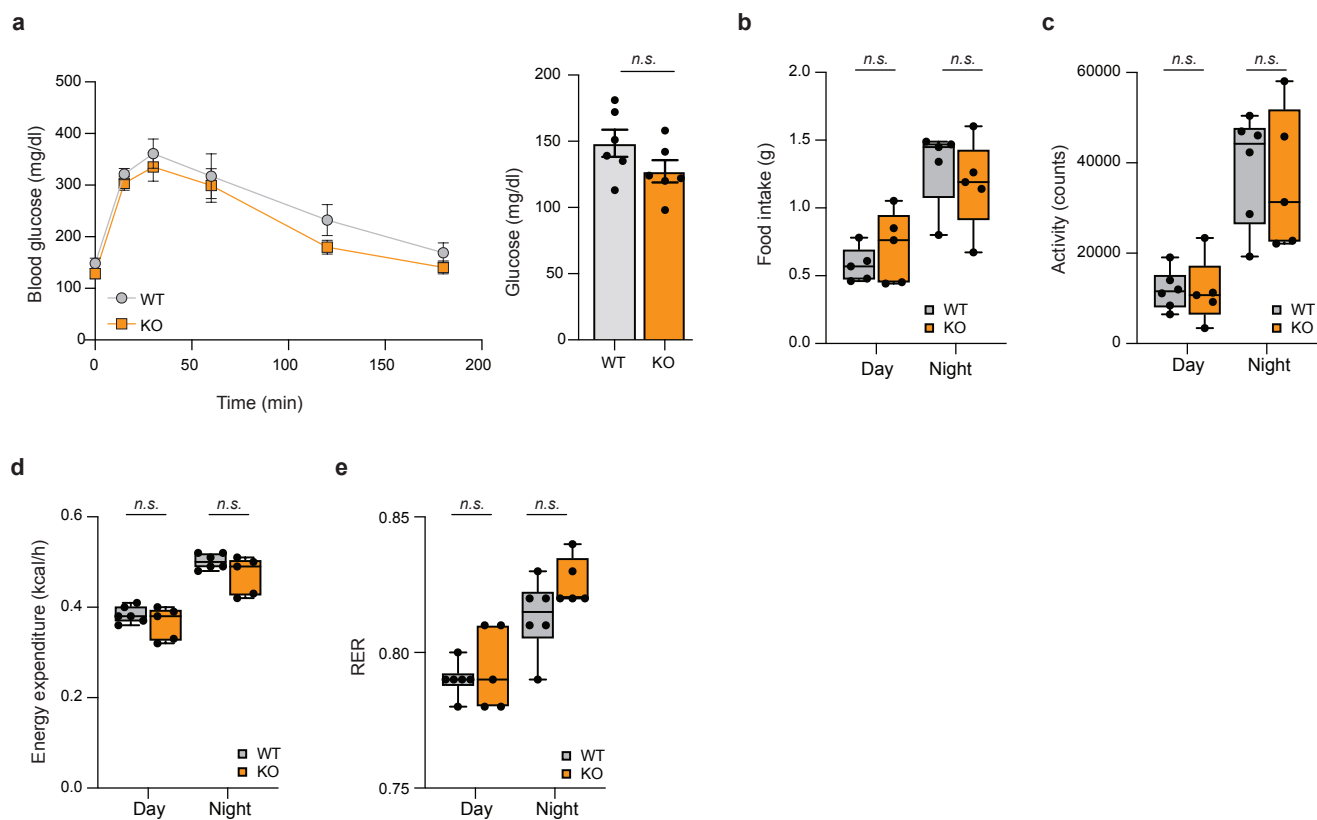
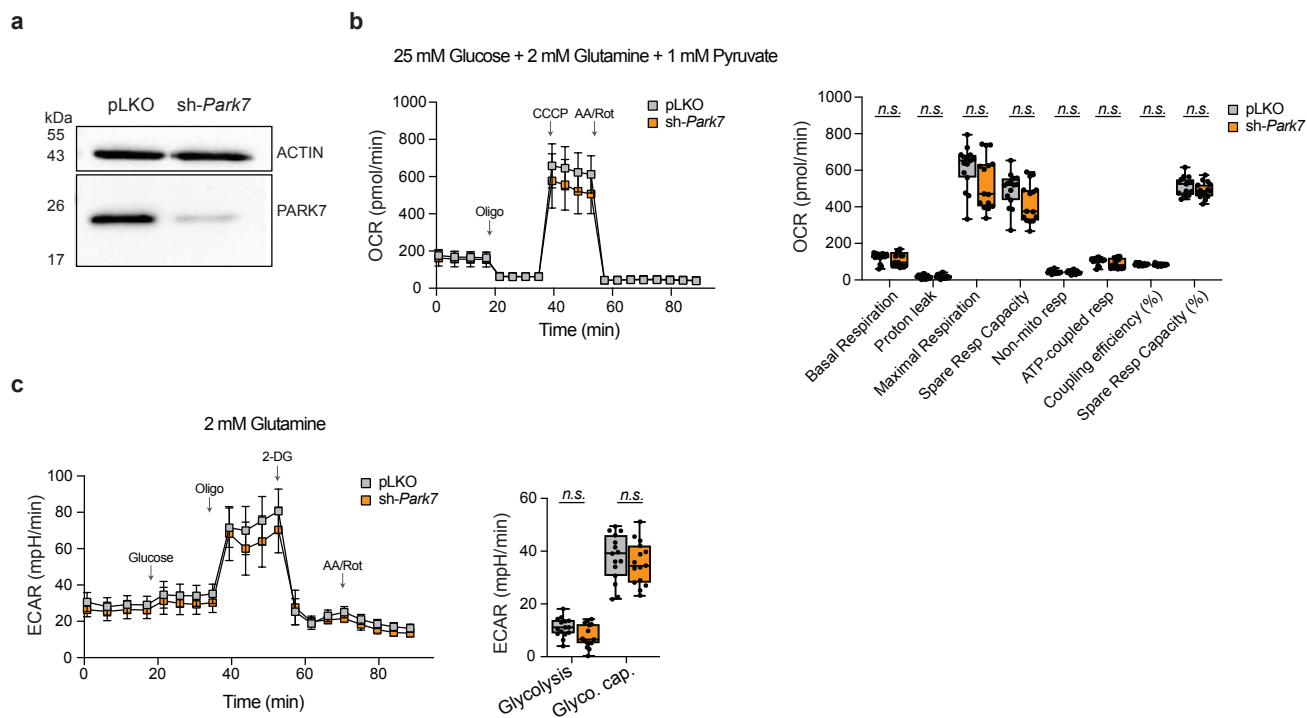


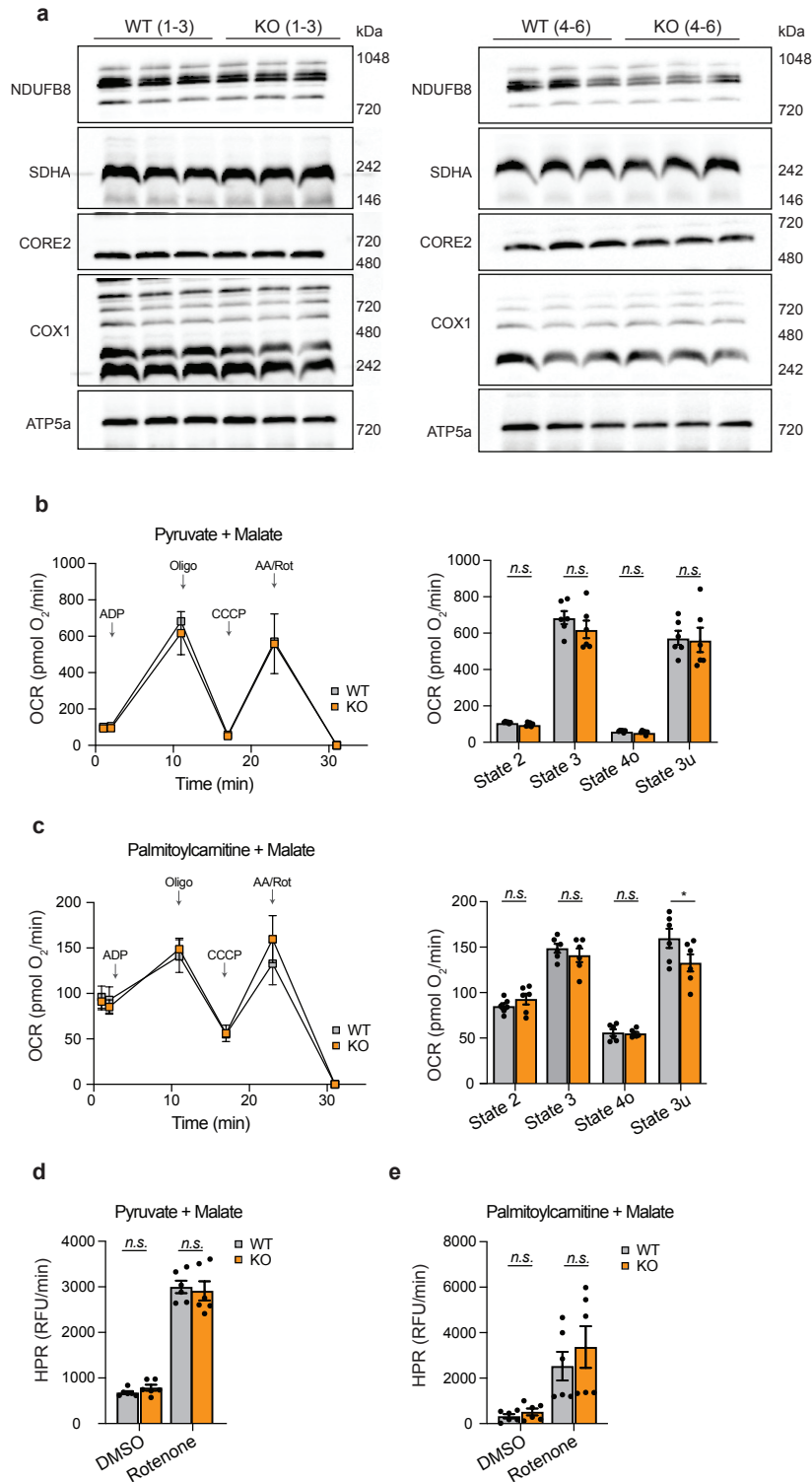
Extended Data Fig. 1: Loss of PARK7 leads to a decrease of fat mass during HFHS diet. Quantification of epididymal (a) and inguinal (b) white adipose tissues (WAT), heart (c), liver (d), and the kidneys (e) from WT and *Park7* KO mice on HFHS diet, as well as gastrocnemius (f), lean mass (g) and fat mass (h) on chow diet. Whiskers show min to max, boxes represent lower and higher quartiles, and middle line as median ($n = 6$) and were analyzed using unpaired t-test. *** $p \leq 0.001$, n.s. not significant.



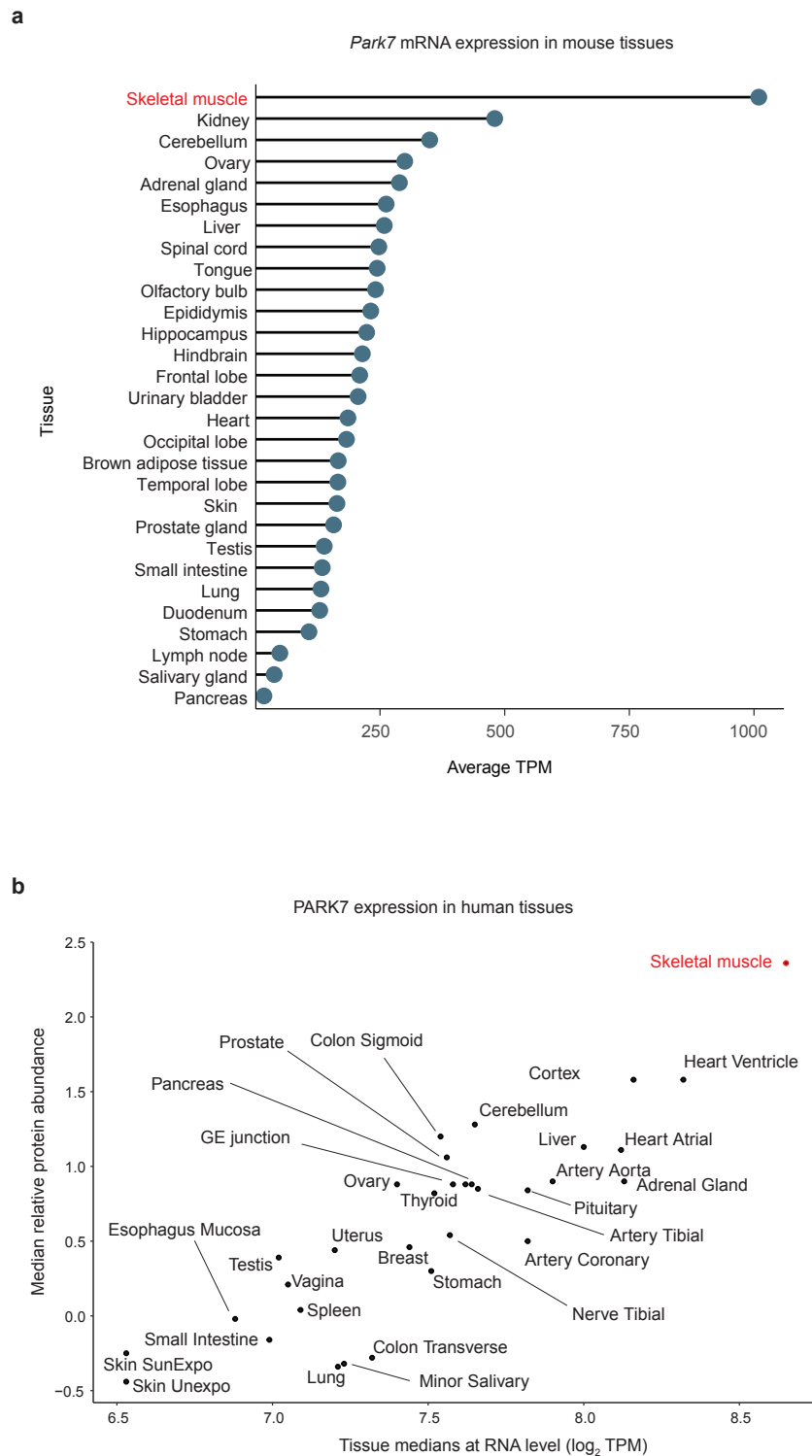
Extended Data Fig. 2: Metabolic phenotyping of *PARK7* knockout mice on HFHS diet. Measurements of (a) glucose tolerance and basal 6h-fasted glucose levels, (b) daily food intake, (c) locomotor activity, (d) energy expenditure, and (e) respiratory exchange ratio (*RER*) from WT and *Park7* KO mice fed a HFHS diet. Data refer to mean \pm SEM, or whiskers showing min to max and boxes showing lower and higher quartiles and middle line as median ($n = 5-6$ per group) and were analyzed using unpaired t-test or two-way ANOVA with Tukey's multiple comparisons test; *n.s.* not significant.



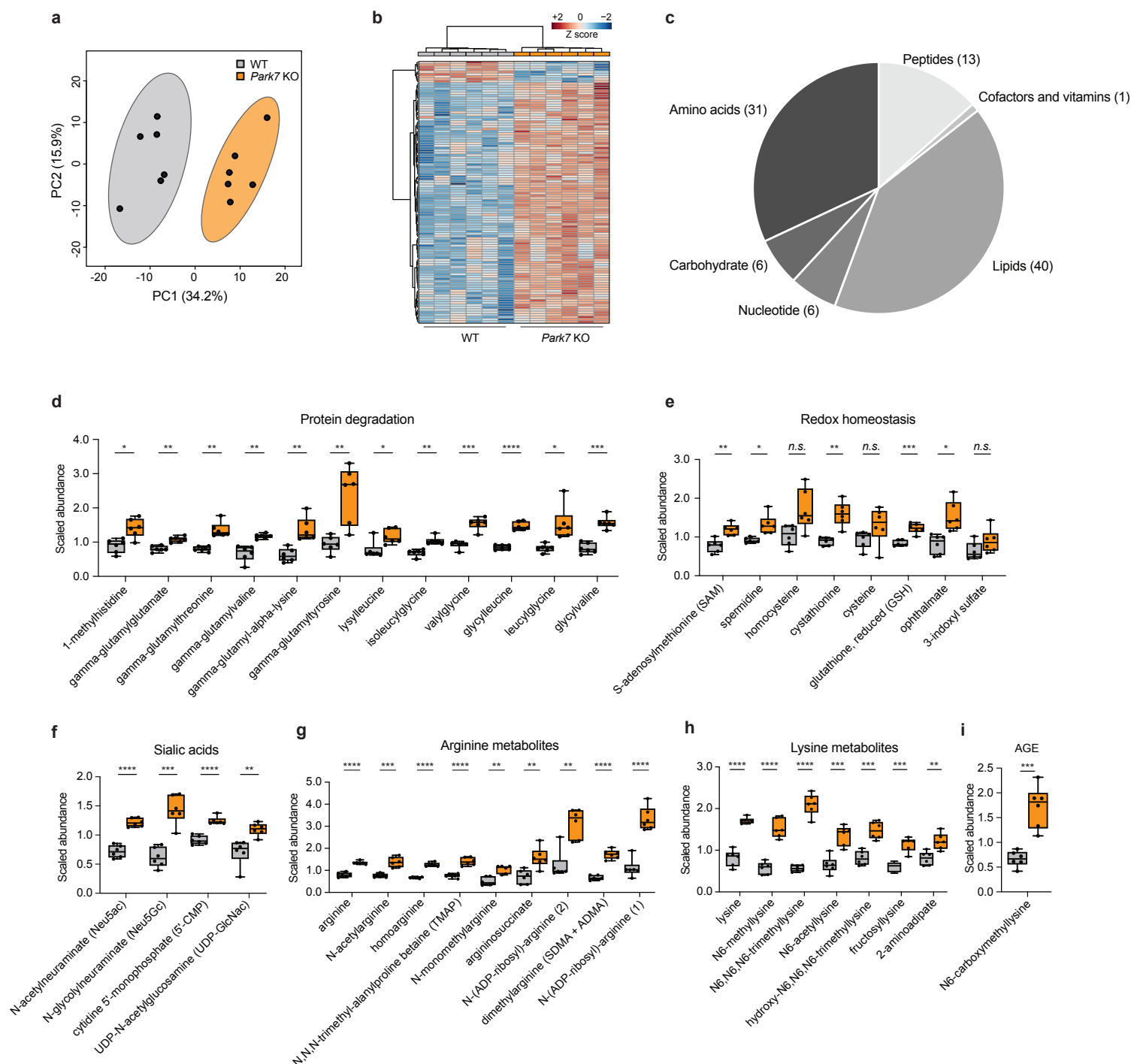
Extended Data Fig. 3: Mitochondrial bioenergetics and glycolytic metabolism are preserved in C2C12 myotubes upon *Park7* loss-of-function. (a) PARK7 abundance in whole cell lysates from C2C12 myotubes infected with single hairpin (sh)-RNAs targeting either empty vector (pLKO) or *Park7* (sh-*Park7*). Actin is used as a loading control. (b) oxygen consumption rate (OCR) average traces (left) and quantification (right) in control (pLKO) and sh-*Park7* C2C12 myotubes (n= 15) in presence of 25 mM glucose/2 mM Glutamine/1 mM Pyruvate after injection of oligomycin (Oligo, 1.5 μ M), CCCP (1.5 μ M), and antimycin A/rotenone (AA/Rot, 4 μ M/2 μ M). (c) Average traces (left) and quantification (right) of extracellular acidification rate (ECAR) in control (pLKO) and sh-*Park7* C2C12 myotubes (n= 15) in presence of 2 mM Glutamine after addition of glucose (10 mM), oligomycin (Oligo, 1.5 μ M), 2-deoxyglucose (2-DG, 100 mM) and antimycin A/rotenone (AA/Rot, 4 μ M/2 μ M). Glyco. cap., glycolytic capacity. Data refer to mean \pm SEM or whiskers showing min to max and boxes showing lower and higher quartiles and middle line as median. Data were analyzed using multiple unpaired t-test with Holm-Sidák multiple comparisons test; n.s., not significant.



Extended Data Fig. 4: Mitochondrial bioenergetics are also preserved in gastrocnemius muscle of *Park7* KO mice. (a) BN-PAGE analysis of respiratory chain complex I, II, III, IV and V level and assembly in mitochondria isolated from gastrocnemius muscles of WT and *Park7* KO mice ($n = 6$). (b) Average traces (left) and quantification (right) of oxygen consumption rate (OCR) by crude mitochondria isolated from gastrocnemius muscles of WT and *Park7* KO mice ($n = 6$) in presence of substrates specific for respiratory chain complex I (10 mM pyruvate/2 mM malate) or (c) beta-oxidation (25 μ M palmitoylcarnitine/2 mM malate). Substrate-dependent respiration (State 2), maximal mitochondrial respiration (State 3), resting respiration (State 4o), and uncoupled respiration (State 3u) are measured in response to 4 mM adenosine diphosphate (ADP), 1.5 μ M oligomycin (Oligo), and 15 μ M CCCP, respectively. Nonmitochondrial respiration is measured upon inhibition of oxidative phosphorylation by 4 μ M antimycin A/2 μ M rotenone (AA/Rot). (d,e) Horseradish peroxidase (HPR)-based quantification of reactive oxygen species produced by mitochondria isolated from gastrocnemius muscles of WT and *Park7* KO mice ($n = 6$) in response to either DMSO (vehicle) or 2 μ M rotenone. RFU, relative fluorescence intensity; Data refer to mean \pm SEM and were analyzed using 2way ANOVA with Sidák's multiple comparisons test (b,c) or two-way ANOVA with Tukey's multiple comparisons test (d,e); * $p \leq 0.05$; n.s., not significant.

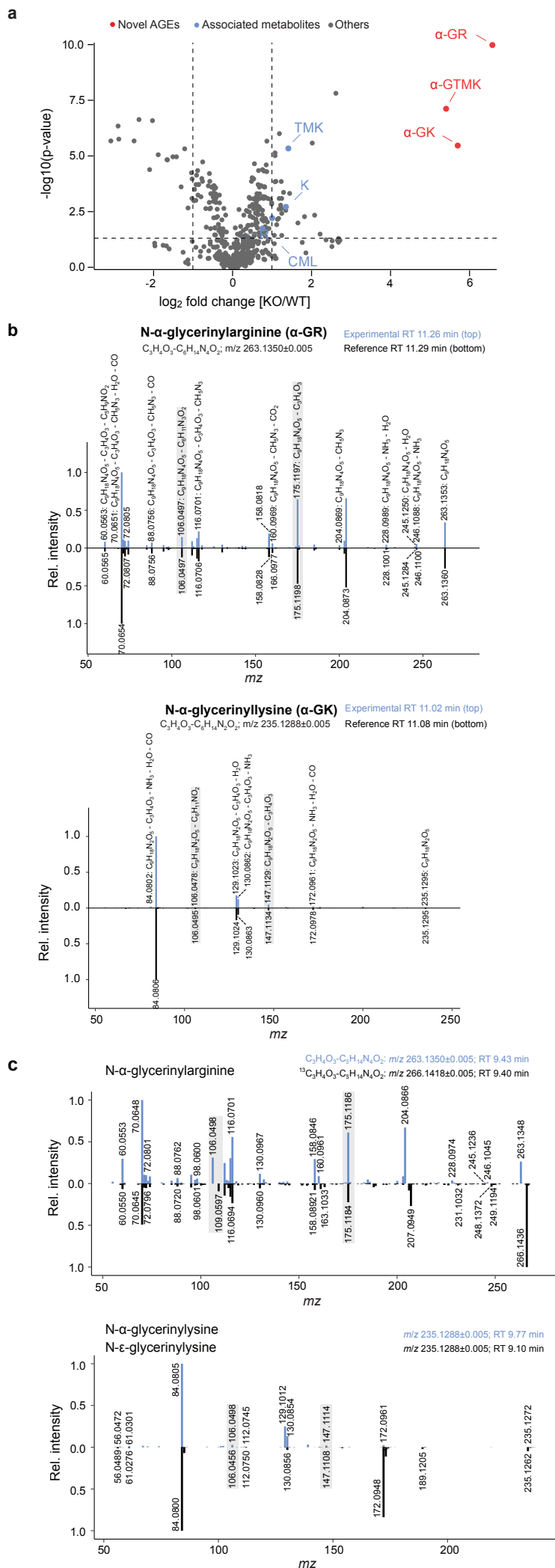


Extended Data Fig. 5: *Park7* is highly expressed in mouse skeletal muscles. (a) Median normalized expression of *Park7* mRNA (Transcripts Per Million, TPM) in mouse tissues (data from <http://www.proteomicsdb.org>). (b) Relative PARK7 protein abundance and *PARK7* mRNA expression (\log_2 normalized; Transcripts Per Million, TPM) in human tissues²⁵.



Extended Data Fig. 6: PARK7-deficiency results in profound alterations of protein and amino acid metabolism, redox homeostasis, and advanced glycation end products. (a) Principal component analysis of untargeted metabolomics data generated by reversed phase-ultrahigh-performance liquid chromatography-tandem mass spectrometry (RP-UHPLC-MS/MS) of gastrocnemius muscles from WT and KO mice on

HFHS diet. (b) Heatmap of 97 metabolites selected by random forest and shown for individual samples. (c) Distribution of selected metabolites in metabolic classes. Metabolite differences largely reflected protein degradation (d), altered redox environment (e), ROS-scavenging sialic acids (f), arginine (g) and lysine metabolites (h), and glycation stress (i). Whiskers show min to max, boxes represent lower and higher quartiles, and middle line is median. Data were analyzed using multiple unpaired t-test with Holm-Sidak multiple comparisons test or unpaired t-test; **** $p \leq 0.0001$, *** $p \leq 0.001$, ** $p \leq 0.01$, * $p \leq 0.05$, n.s. not significant.



Extended Data Fig. 7: Structural confirmation of the new glycerinyll-AGEs. (a) Volcano plot comparing metabolomes of gastrocnemius from WT and KO mice under chow diet. (b) Structural verification with commercially synthesized authentic standards N- α -glycerinyllarginine ($\alpha\text{-GR}$) and N- α -glycerinylllysine ($\alpha\text{-GK}$). (c) Confirmation of structures by comparison with D-glucose- $^{13}\text{C}_6$ isotopically labeled N- α -glycerinyllarginine ($\alpha\text{-GR}$) and commercially synthesized N- ϵ -glycerinylllysine ($\epsilon\text{-GK}$).